Geophys. J. Int. (1992) **109**, 565–580

Palaeomagnetic dating of fault rocks: evidence for Permian and Mesozoic movements and brittle deformation along the extensional Dalsfjord Fault, western Norway

T. H. Torsvik,[1,2] B. A. Sturt,[1] E. Swensson,[3] T. B. Andersen[3] and J. F. Dewey[2]

[1] *Geological Survey of Norway, PB* 3006 *Lade, N-*7002 *Trondheim, Norway*
[2] *Department of Earth Sciences, University of Oxford, Oxford* OX1 3PR, *UK*
[3] *Department of Geology, University of Oslo, PO Box* 1047, *Blindern,* 0316 *Oslo, Norway*

Accepted 1991 December 5. Received 1991 December 5; in original form 1991 September 26

SUMMARY

Palaeomagnetic and structural studies of the Dalsfjord Nappe, western Norway, show that the basal low-angle detachment (Dalsfjord Fault) is a long-lived fault zone, and that the most important phase of faulting was of Devonian extension, probably nucleated on an earlier Silurian (Scandian) thrust. Fault rocks produced during subsequent movements indicate that the Dalsfjord Fault underwent periods of brittle low-angle extensional reactivation during the Permian (250–260 Ma) and Upper Jurassic/Lower Cretaceous (*c.* 150 Ma), corresponding with stages of major extensional movements on the continental shelf. Palaeomagnetic studies may be of great importance for dating faults and major movement stages in long-lived fault systems. The particular importance of the results is that they show that low-angle normal faults can operate in a brittle upper crustal regime.

Key words: deformation, faulting, palaeomagnetism, Norway.

INTRODUCTION

In the West Norwegian Caledonides, low-angle faults have been interpreted as thrusts (Høysæter 1971; Nilsen 1968; Roberts 1983; Sturt 1983; Torsvik *et al.* 1986), as normal faults forming part of a *single* Lower to Middle Devonian detachment (Hossack 1984; Norton 1986; Seranne & Seguret 1987; Seguret *et al.* 1989), or as an array of extensional detachments (Andersen & Jamtveit 1990). Inherent in the extensional models, the transition from ductile to brittle deformation and faulting reflects retrograde *Devonian* extensional deformation coincident with uplift.

A later phase of Late Devonian/Early Carboniferous north–south shortening has been advocated by some workers (Sturt 1983; Roberts 1983; Torsvik *et al.* 1986, 1987, 1988) to explain the complex geometry developed in both hanging-wall and foot-wall lithologies, particularly close to tight east–west trending folds in footwall metamorphic rocks. Torsvik *et al.* (1988) also suggested that some characteristics of the inferred Early–Middle Devonian extensional deformation, could prove to have a Late Palaeozoic–Mesozoic origin.

Studies of fault rocks provide a direct technique in dating major phases of fault movements or rejuvenation; both radiometric and/or palaeomagnetic methods have been applied (e.g. Grønlie & Torsvik 1989; Roddom, Miller & Flinn 1989). In this paper, we describe an application of the palaeomagnetic dating of fault rocks. The success and precision of the palaeomagnetic technique requires several assumptions and requirements to be satisfied as follows:

(1) that the structural grain does not affect remanence acquisition (deflection);

(2) that the results may be compared with well-defined reference data or an established apparent polar wander (APW) path;

(3) that unaccounted-for post-acquisitional structural rotations are precluded;

(4) that an appropriate sampling strategy is used to provide constraints on the relative ages of magnetization components; and

(5) that the observed magnetic minerals relate to mineral growth during significant fault displacement rather than later fluid movements along the same fault zone.

Here, palaeomagnetic and magnetic fabric data from brittle fault rocks are reported in an attempt to provide a time framework to the complex history of the Dalsfjord Fault (Fig. 1).

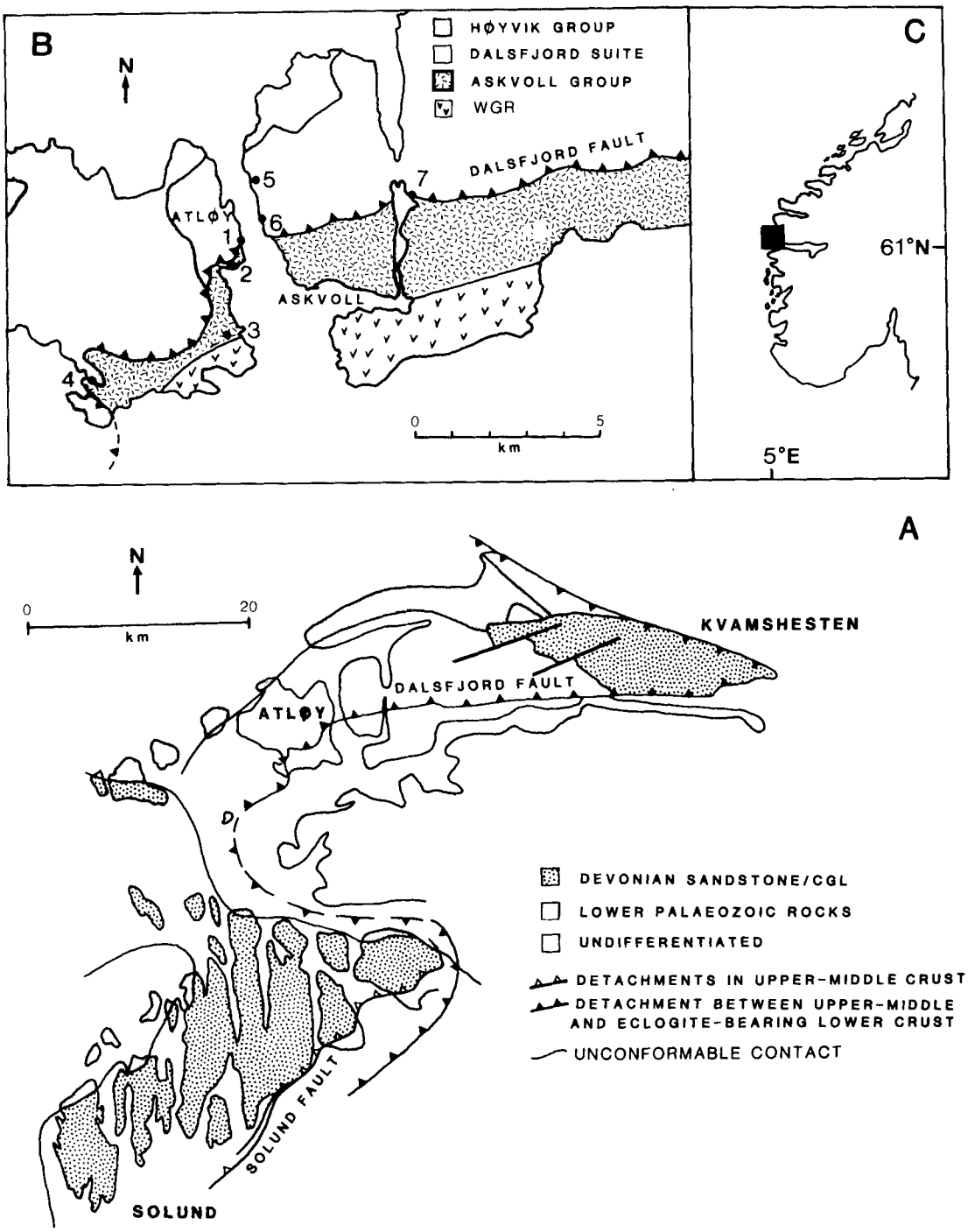

Figure 1. (a) Geological sketch-map of the Sunnfjord area, Western Norway, showing the Dalsfjord and Solund Faults. Simplified from Andersen & Jamtveit (1990). (b) Geological sketch-map of the Atløy–Askvoll area. Numbers refer to palaeomagnetic sampling sites. WGR = Western Gneiss Region. (c) Southwestern Norway (Sunnfjord area is indicated as a solid box).

THE DALSFJORD FAULT

The Dalsfjord Fault (Fig. 1) forms the southern segment of the Kvamshesten Detachment Zone (Andersen & Jamtveit 1990). The Fault separates hanging-wall rocks of the Dalsfjord Nappe comprising Precambrian gneisses, on which later cover sequences of Cambro-Silurian and Devonian age repose, from thick foot-wall mylonites of the Askvoll Group and the Western Gneiss Region (Skjerlie 1969, 1971, 1974; Brekke & Solberg 1987; Andersen *et al.* 1991). The Devonian rocks of Kvamshesten occur in the eastern part of the Dalsfjord Nappe (Fig. 1a) where they rest partly unconformably on the Precambrian rocks of the Dalsfjord Suite or directly with faulted contact, on the foot-wall. The Dalsfjord Fault rises from sea-level in the west (Fig. 1a) to intersect the unconformity at the base of the Devonian and

the rocks of the Dalsfjord Suite, and continues eastward forming a base to the Devonian sediments. Along the northern margin of the Kvamshesten Massif, the detachment zone is marked by about 2 km of thick mylonites in the footwall. Along the Dalsfjord Fault, brittle movements produced a variety of fault breccias and, finally clay gouges in the hanging-wall. At Kvamshesten the detachment zone is folded in a roughly symmetrical open east–west trending syncline, a style that is in marked contrast to the more intense folding of the Devonian sediments (Torsvik *et al.* 1986).

PALAEOMAGNETIC SAMPLING OF THE DALSFJORD FAULT ROCKS

A total of seven sites were examined from the island of Atløy (sites 1–4) and the district of Askvoll (sites 5–7, Fig. 1b, Table 1). At Atløy, the Dalsfjord Fault is marked by a conspicuous zone of variably brecciated rocks, which may exceed 50 m in thickness in the hanging-wall. The fault zone separates quartz syenitic gneisses of the Dalsfjord Suite and its probable Eo-Cambrian cover sequence (Høyvik Group) from the footwall lithologies of the Askvoll Group. The Askvoll Group is a strongly non-coaxially deformed sequence of greenstones, metagabbros, amphibolites and metasedimentary rocks with a maximum structural thickness of about 2 km. The penetrative mylonitic fabrics (site 3, Fig. 1b) in these rocks were developed during retrograde metamorphism related to the uplift during the orogenic extensional collapse in Late Silurian–Early Devonian times (Andersen & Jamtveit 1990; Swensson & Andersen 1991). The upper part of the fault zone is characterized by intensely brecciated hanging-wall rocks forming a typical network fault breccia (sites 1a and c). The dark green matrix of the breccia is made up of fine-grained epidote and chlorite and contains small fragments of previously brecciated and cataclastic material. The zone of brecciation may extend up into the hanging-wall for some 50–100 m (sites 5 and 6) across which there is a progressive decrease in the intensity of brecciation. Angular and irregular fragments of the foliated syenitic protolith may reach several metres in the upper part of the brecciated zone. Along the road-section where the most detailed palaeomagnetic sampling was carried out (site 1a), the blocks are derived from already brecciated orthogneisses and cataclasites of the overlying Dalsfjord Suite (Brekke & Solberg 1987). Below a red breccia at site 1, a thin zone of brecciation is also found in the underlying mylonites. Further brecciation along the Dalsfjord Fault may be observed at various places (e.g. site 7), and within the southern part of the Kvamshesten area, though this has not been observed on the northern limb of the Kvamshesten syncline (Torsvik *et al.* 1986).

The Dalsfjord Fault zone has a complex history as shown by later reactivation marked by a conspicuous 20 cm red-coloured fault breccia (site 1b), located at the base of the cataclasite zone in the hanging-wall. Locally, late movements are also indicated by the development of pale green clay-bearing fault gouges (site 7b). The red breccia (site 1b) contains small fragments of the green cataclasite and has a matrix of finely comminuted fragments, rock flour and clays; later fractures contain expanding clays. The breccia is a compact highly indurated rock, cut by a number of small normal faults with small displacements. The red breccias and clays are important in that they show that the low-angle extensional displacements occurred at shallow levels in the oxidizing zone.

LABORATORY EXPERIMENTS

The natural remanent magnetization (NRM) was measured on a two-axis Squid magnetometer (Oxford University) and a Molspin magnetometer (Bergen University). 140 samples were subjected to thermal, and to a lesser extent, alternating field (AF) demagnetization. Characteristic remanence components were calculated by least-square analyses. The anisotropy of magnetic susceptibility was further studied for 91 samples using a low-induction susceptibility bridge (KLY-2, Bergen University) or a Minisep delineater (Oxford University) calibrated against the former instrument.

Table 1. Magnetic fabric results.

Site	Height(m)	Eigenvalues e1	e2	e3	%An	Eigenvectors Kmax D°/I°	Kmin D°/I°
Atløy							
1a HW Breccia	(0.1-1.3)	1.0402	1.0199	0.9740	6.8	097/68	269/21
Contact		1.0035	1.0010	0.9935	1.0	331/19	173/66
1b Red Breccia		1.0028	0.9978	0.9912	1.2	303/17	144/70
1c FW Breccia	(0.85-1.65)	1.0768	1.0206	0.9015	19.5	289/6	180/73
2 FW Greenstone	(c.50)	1.0461	0.9987	0.9433	10.9	268/11	167/41
3 FW Mylonite	(c.100)	1.3738	0.9894	0.6361	117.9	283/6	183/57
4 Breccia		1.0243	1.0078	0.9662	6.0	333/15	212/72
Askvoll							
5 HW Breccia	(c.100)	1.0167	1.0108	0.9909	2.6	337/8	115/78
6 HW Breccia	(c.50)	1.0813	0.9923	0.9106	18.9	320/34	145/49
7a HW Breccia	(2.0-3.0)	1.0164	0.9921	0.9411	8.1	090/53	344/14
7b Green Fault-gouge		1.0135	1.0061	0.9959	1.7		
7c FW Breccia	(0-0.3)	1.0080	0.9920	0.9759	3.3	333/31	190/51

e1,e2,e3=principal eigenvalues; %An=(K_{max}/K_{min}-1)*100;
D°/I°=declination/inclination for eigenvectors;
FW=Footwall; HW=Hangingwall; Approximate height in metres above (HW) and below (FW) the Dalsfjord Fault.

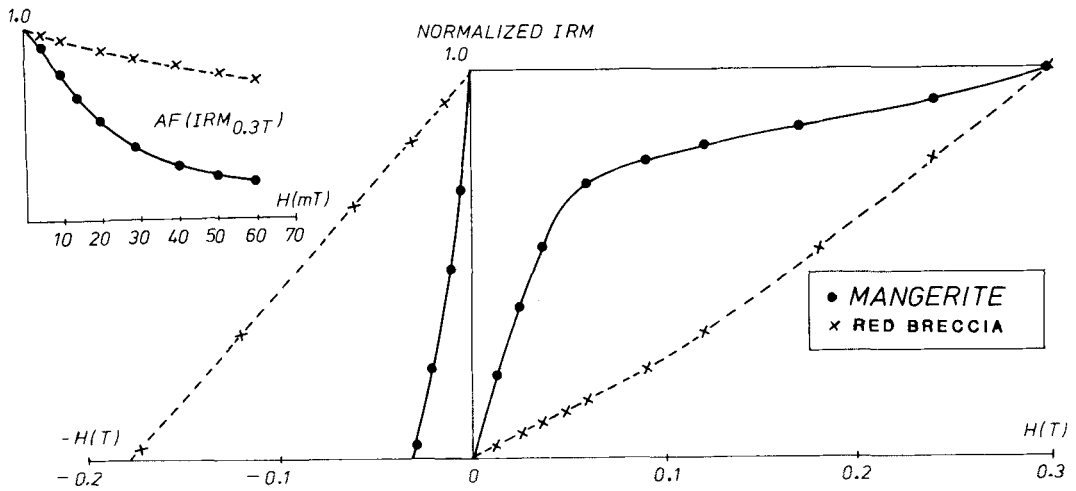

Figure 2. Typical isothermal magnetization (IRM) curves and AF demagnetization spectra (IRM: 0.3 T) for the late red breccia (crosses—site 1b) and hanging-wall mangerite breccia samples (dots—site 1a). H(T) = magnetizing field in Tesla.

Opaque mineralogy

Petrographic studies show that hanging-wall brecciated mangerites and foot-wall greenstones are dominated by magnetite with accessory haematite and pyrrhotite. Thermal decay curves (see below), however, indicate that magnetite appears to be the most influential remanence-carrying mineral phase in all hanging-wall and foot-wall lithologies. In the case of the red breccia (site 1b), Curie temperatures approaching 580 °C and 680 °C, and isothermal remanent magnetization (IRM) curves combined with demagnetization studies (see below), show that magnetite and haematite are the principal remanence carriers. The late red breccia has a red haematite and goethite stained matrix with abundant pyrrhotite and accessory magnetite. IRM curves are dominated clearly by the high-coercivity mineral phases (Fig. 2). Secondary magnetite is commonly produced during heating and reflected as an increase in bulk susceptibility (Fig. 3). Separation of matrix and clasts in the red breccia show that magnetite formation is essentially at the expense of matrix minerals (Fig. 3). Haematite Curie temperatures were not observed in clasts. Within the matrix, goethite, as observed in thin sections, may have originated partly by weathering, whereas haematite was formed clearly through precipitation relating to metasomatic fluid fluxes.

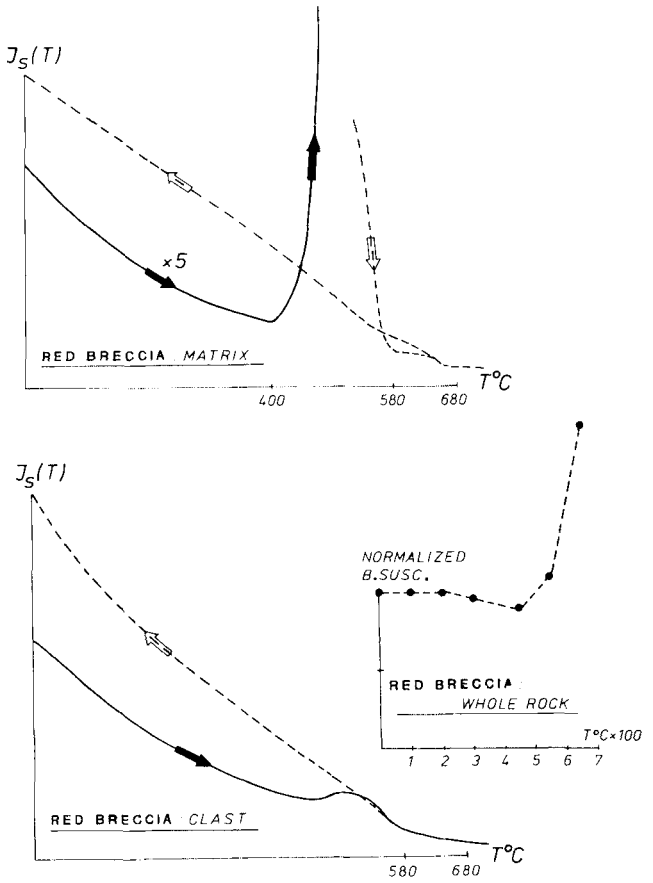

Figure 3. Thermomagnetic curves [$J_s(T)$] for a sample from the late red breccia. Secondary production of magnetite, in part oxidized to haematite, is most profound in the matrix (heating curve is drawn 5 times expanded relative the cooling curve). Magnetite production (whole rock) is indicated also by the large increase in bulk susceptibility (inset).

The magnetic fabrics and structural data

The anisotropy of magnetic susceptibility (AMS) ellipsoids varies systematically across the Dalsfjord Fault zone. Specimens of brecciated mangerite from the hanging-wall of site 1a (Fig. 4a) are dominated by steeply dipping and near north–south striking magnetic foliation planes (K_{max}–K_{int}) with easterly (097°) steeply plunging lineations (K_{max}). The AMS ellipsoids are oblate with anisotropies [$\%An = (K_{max}/K_{min} - 1) \times 100$] ranging between 4 and 12 per cent (Fig. 5, Table 1). Approximately 30 cm above the red breccia, $\%An$ decreases systematically, and within 10 cm of the red breccia, the steeply dipping foliation is replaced by a gently inclined foliation with northwest-trending lineations. This fabric compares with a gently inclined magnetic foliation with lineations trending northwest (303°), developed in the late red breccia (see also Table 1). The magnetic fabric in the red breccia, however, is almost isotropic, $\%An$ averages to approximately 1 per cent (Fig.

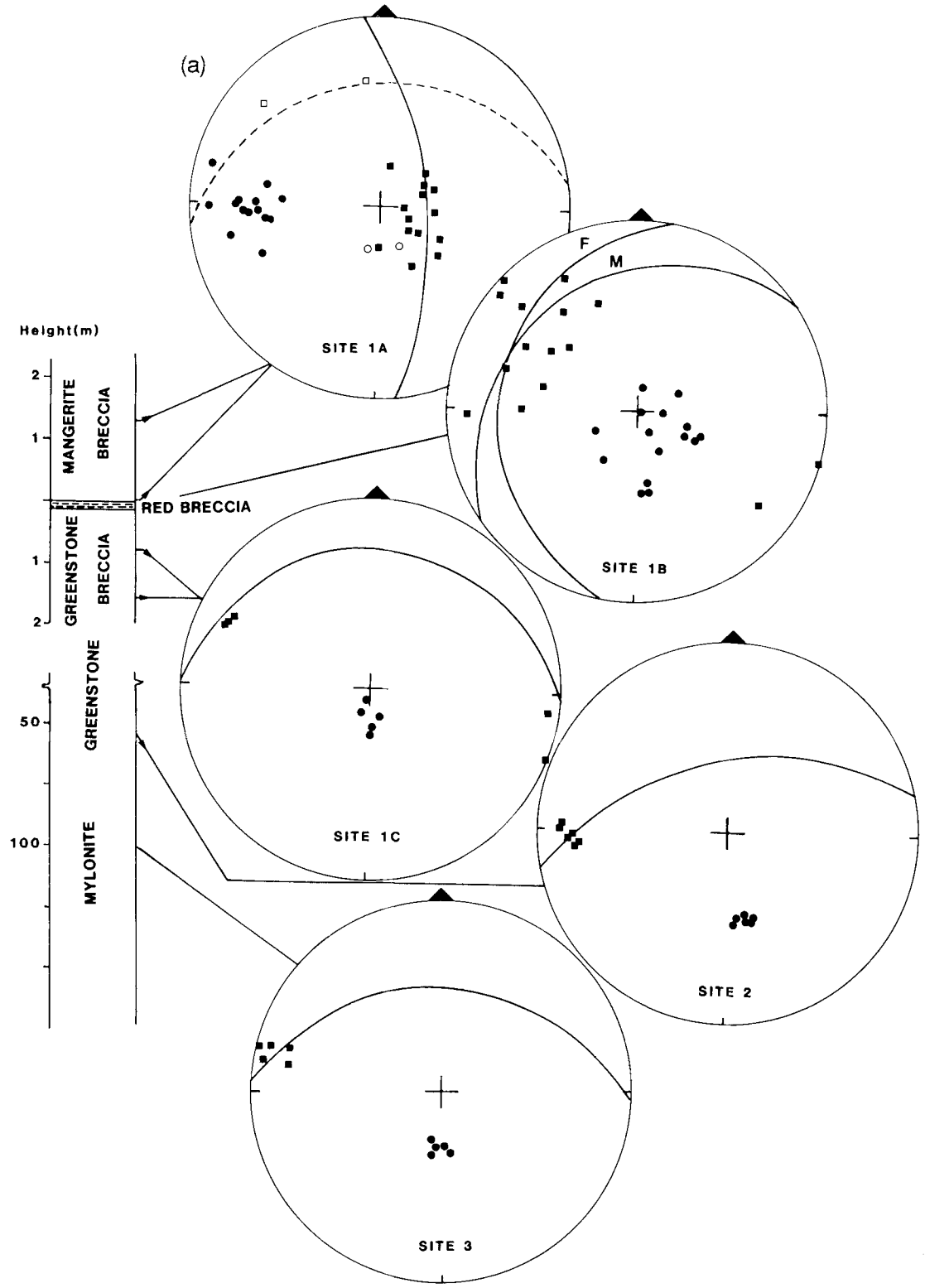

Figure 4. (a) Vertical section showing the Askvoll Group (foot-wall) and the Dalsfjord Suite (hanging-wall) separated by the Dalsfjord Fault. In lower hemisphere equal-angle stereoplots, K_{min} (solid circles) and K_{max} (solid squares) for individual samples are shown together with the best fitted magnetic foliation planes. Stippled great-circle and open symbols for site 1A refer to two contact specimens against the late red breccia (downward dipping). For site 1A, F and M refer to fault contact orientation and magnetic foliation plane respectively. (b) Lower hemisphere poles to mylonitic foliations (solid circles) and megascopic stretching lineations (solid squares) measured within the Askvoll Group (foot-wall). Best fitted great circle for foliation poles $-005°/+81°$ ($N = 88$). Lineations average to $276°/+12°$ ($N = 27$, 95 per cent error confidence circle $= 3.8$).

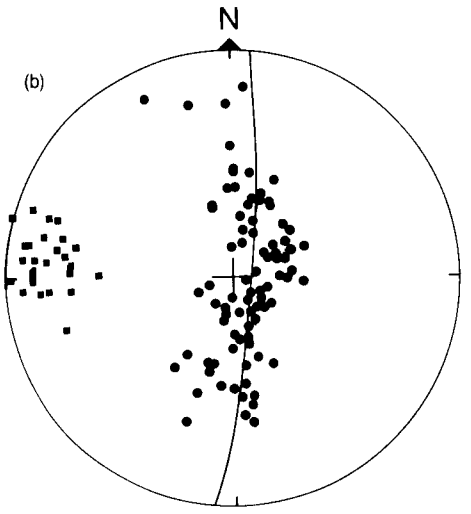

Figure 4. (b)

5), and the poorly developed magnetic foliation does not agree fully with the strike and dip of the fault (235/18°NW, Fig. 4a). The fabrics from the red breccia closely correspond to fabrics obtained from site 4.

Brecciated rocks in the foot-wall (site 1c) are dominated by east–west striking magnetic foliation planes, oblate magnetic ellipsoids, and pronounced stretching lineations (Fig. 4a) trending 289°. The *%An* approximates to 20 per cent about 1.5 m below the red breccia, and decreases towards the red breccia (note that open circular symbols in Fig. 5 represent data from site 7c).

Foliated greenstones about 50 m below the Dalsfjord Fault also have east–west magnetic foliation planes, which are more steeply dipping and with subhorizontal westerly trending lineations (Fig. 4a). *%An* is approximately 11 per cent (Table 1). *%An* and flattening strain in brecciated or foliated foot-wall rocks is *dramatically* lower than that recorded from *mylonitic* greenstones from site 3 (mean $\%An = 118$ per cent), i.e. at about 100 m below the Dalsfjord Fault. However, the orientation of the principal susceptibility axes remains nearly constant through the foot-wall at Atløy (compare sites 2 and 3 in Fig. 4a).

The magnetic fabrics in the foot-wall (Askvoll Group) closely correspond to mylonitic foliations and stretching lineations. Stretching lineations average to 276°/12° (Fig. 4b), which agree with magnetic lineations from sites 2 and 3 (Fig. 4a, Table 1). Poles to mylonitic foliations from the Askvoll group display a north–south girdle, hence defining east–west folding with a gentle westerly plunge (Fig. 4b). The folding of the Askvoll Group extensional mylonites and the Kvamshesten Devonian rocks (Torsvik *et al.* 1986) is coaxial.

At site 7a (Askvoll, Table 1), the magnetic fabric pattern compares with those of the Atløy sites (site 1). Again, the hanging-wall is dominated by steeply inclined foliation planes with steep eastward plunging lineations (Fig. 6). The *%An* is approximately 8 per cent (Table 1). The later clay-bearing fault gouge (site 7b) is almost isotropic ($\%An = 1.7$) and no directionally consistent foliations or lineations are observed. On the other hand, the foot-wall rocks show east–west foliation planes dipping about 45° toward the north. At this locality, the Dalsfjord Fault dips 50° toward the north-northwest (strike =289°); hence, in this area, the youngest fault rupture with the formation of clay-bearing fault gouges (site 7b), follows the pre-existing foliation in the older foot-wall breccias. The *%An* in the foot-wall is approximately 3 per cent. Magnetic lineations are northwesterly directed and compare with breccia lineations seen from sites 1b–c and 4, and with hanging-wall breccias of sites 5 and 6. Conversely, the older foot-wall fabrics (sites 2 and 3) are characterized by westerly plunging lineations (Figs 4a, b and 6).

Palaeomagnetic data

Characteristic remanence components and average NRM intensities from a profile through the Dalsfjord Fault zone (site 1) are shown in Fig. 5. The breccias in the foot-wall and hanging-wall, derived from mylonitic greenstones and mangerites respectively, have negative inclined high unblocking (HB) temperature components, denoted A2, with southwest declinations (Figs 5 and 7). Superimposed low unblocking (LB) temperature components are present but commonly these proved difficult to estimate because of some irregular demagnetization behaviour (*cf.* Fig. 7a), and in part due to overlapping thermal stability spectra. Some samples, however, display a well-defined LB component with north-northwest declinations and steeply downward-dipping inclinations (*cf.* Figs 5 and 7b). This component, denoted A1, forms the HB temperature component observed in the younger reddened fault breccia (Figs 5 and 8), hence indicating a 'positive contact test' with respect to component A1. In the red breccia, magnetite and haematite appear to be the main remanence carriers, but pyrrhotite and goethite are also potential remanence carriers. The presence of goethite may be indicated by a substantial drop in NRM intensity below 150 °C. The demagnetization trajectory below 150 °C commonly proved different from that of the high unblocking temperature range (see Figs 8a, c). Thermal decay curves indicate a predominance of unblocking temperatures below 580 °C but remanence stability is retained up to 670 °C (Fig. 8a). The red breccia remanence is incompletely demagnetized by the alternating field (AF) method (Fig. 8b); median destructive fields range between 60 and 80 mT. Red breccia samples from the upper contact against the hanging-wall indicated the presence of both normal and reverse field directions at the sample level. The reverse field direction was always isolated at high temperatures and is resident in haematite (Fig. 8d). Within the contact of the hanging-wall breccias, a few samples also indicate the presence of this reverse polarity direction but only in one sample was this reverse polarity 'red breccia' magnetization properly isolated (*cf.* stereoplot in Fig. 5). A peak in NRM intensities along the upper contact of the red breccia is observed also, as is a gradual decrease in NRM intensity upsection (Fig. 5). Measurements on certain samples within the central part of the red breccia also suggest the presence of a high blocking normal polarity direction due to pronounced off-origin trajectories (Fig. 8c) but the underlying component was not identified.

At site 2, foliated greenstones display a similar component structure to the network breccias of site 1, and at this site *all* samples delineate LB components (A1) of fairly high quality below 175°–200 °C (Fig. 7b). Non-

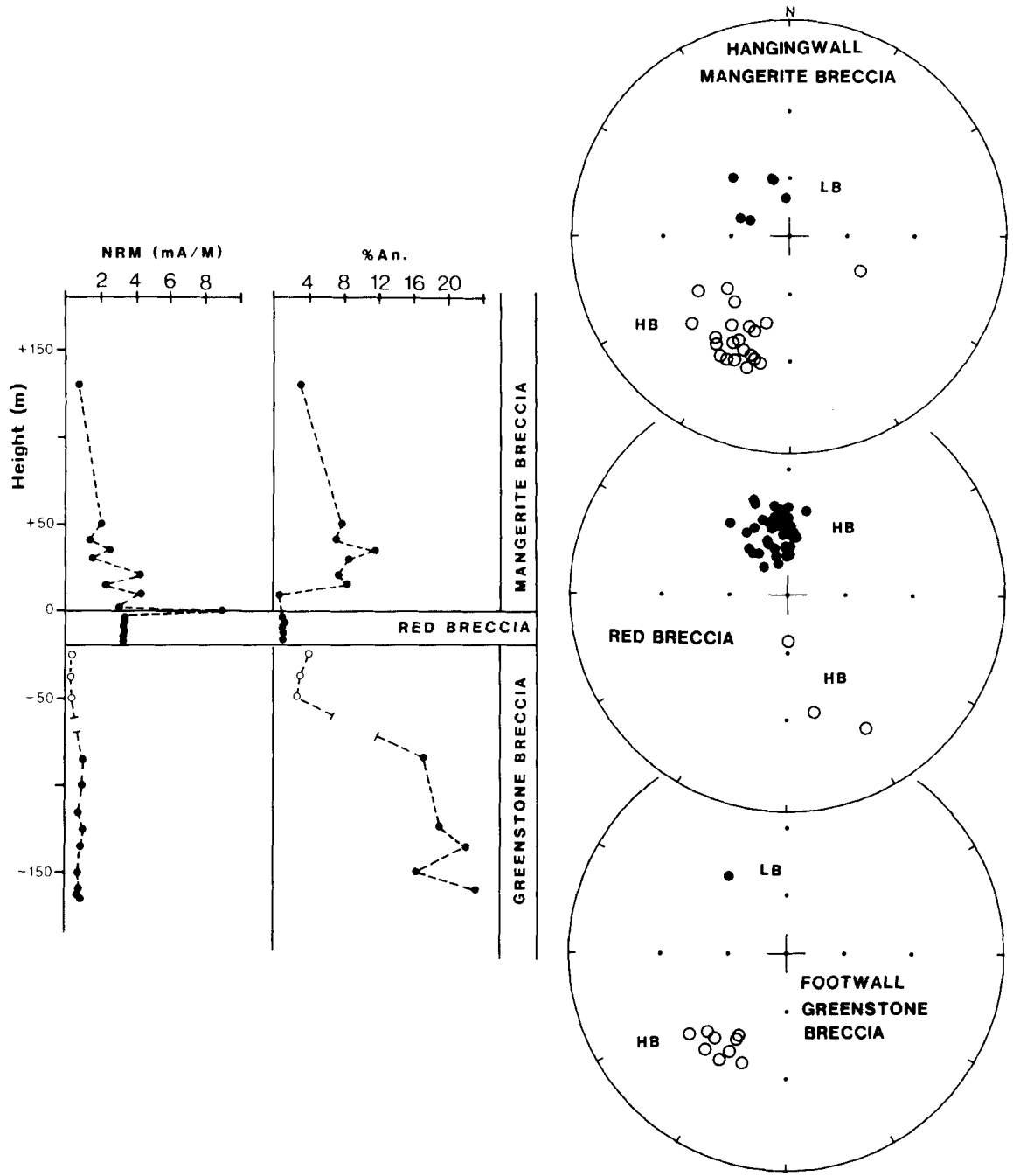

Figure 5. Characteristic remanence components, NRM intensity and percentage anisotropy obtained from the mangerite breccia (Dalsfjord Suite—site 1a), the red breccia (site 1b) and the greenstone breccia (Askvoll Group—site 1c). In equal-angle stereoplots, closed (open) symbols represent positive (negative) inclined inclinations. LB and HB denote low unblocking and high unblocking components respectively.

overlapping blocking spectra may indicate partial thermoremanent (PTRM) overprinting. Hanging-wall rocks of site 5, about 100 m above the fault, have component A2 (Fig.9a) although, as the fault is approached (site 6), both components (A1 and A2) can be discerned clearly (Fig. 9b). For the latter sites, however, the high blocking A2 component did not decay towards the origin of Zijderveld diagrams and hence, an underlying component appears to be present (Fig. 9). Unfortunately the occurrence of viscous behaviour at high temperatures precludes confident identification of the underlying component, which may be of pre-A2 origin.

From site 7, it proved difficult to isolate remanence components in both the hanging-wall rocks and the clay-bearing fault gouge. The fault gouge appeared to be dominated by steep downward pointing remanences with northerly declinations, probably of recent origin. The immediate foot-wall provided remanence directions conforming to component A2.

No remanence components were delineated from site 4

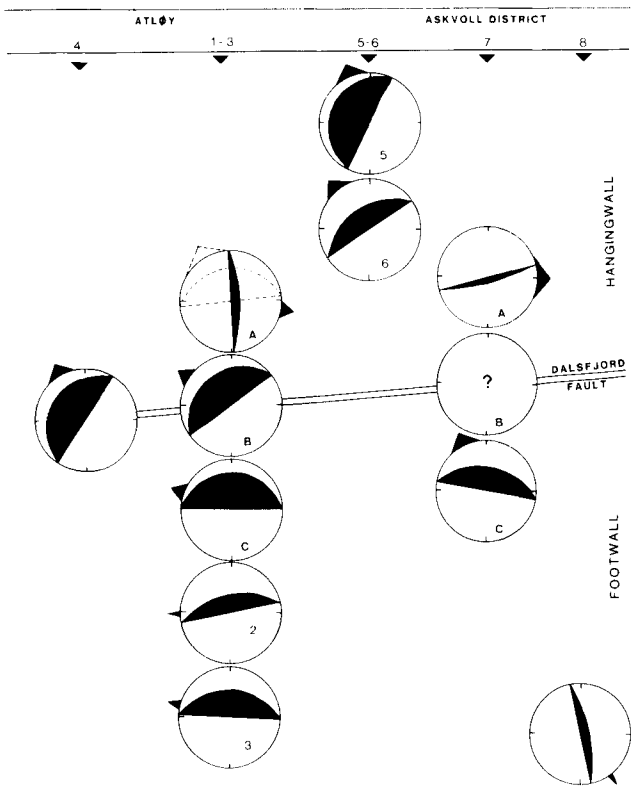

Figure 6. Stereoplots of magnetic foliation planes and lineations when showing within-site consistency (arrows with 95 per cent confidence circles) for sites 1 to 7. Stippled plane for site 1a refers to contact samples (see Fig. 4a).

due to unstable directional behaviour. From mylonitic foot-wall samples of site 3, it is possible to observe subhorizontal remanence components with westerly declinations closely duplicating the orientation of K_{max}, and apparently governed by the strong structural grain ($\%An = 118$ per cent).

INTERPRETATION

Characteristic remanence components from fault rocks associated with the development of the Dalsfjord Fault form two distinct remanence groups, A1 and A2 (Fig. 10, Table 2). Apart from site 3 (excluded), no relationship with either the direction or magnitude of the magnetic susceptibility ellipsoid is observed; therefore, remanence directions are apparently unrelated to strain effects associated with the development of the breccias.

Group A2 is the characteristic high-temperature component in the breccias of the hanging-wall and foot-wall (sites 1a, b, 5–6 and 7c). A2 is identified also within foliated greenstones at some distance from the Dalsfjord Fault (site 2), however, and consequently, it is not possible to preclude regional overprinting as opposed to a fault-related breccia 'formation' origin, which the authors prefer. However, network breccias close to Dalsfjord Fault are completely overprinted by the A2 magnetization, whereas samples higher up in the hanging-wall (sites 5 and 6) clearly carry an underlying and presumably older remanence component. With reference to Atløy, group A2 implies a palaeolatitude of 18°N (Fig. 12b), and a comparison with available palaeomagnetic data from Europe (Torsvik *et al.* 1990, 1992) demonstrate that group A2 remanences have a Permian age (Fig. 12a). A Permian age for the group A2 remanence is sustained from a comparison with Permian data from the Oslo Rift and numerous dykes in coastal Western and Central Norway providing similar directional results (*cf.* Torsvik *et al.* 1989, 1992).

Group A1 forms the characteristic magnetic signature of the late red fault breccia, but also conforms to the low blocking temperature components in the older green breccias, notably in the *hanging-wall.* Petrographic studies reveal that red-coloured breccia matrix also infills millimetre-scale microfractures in the hanging-wall rocks. Along the contact to the hanging-wall, the group A1 remanence is superimposed on its assumed normal polarity counterpart, which suggests a change in polarity of the geomagnetic field, probably from reverse to normal, during the earlier formation of the red breccia. Group A1 gives a palaeolatitude 39°N (Fig. 12b) and is arguably of Upper Jurassic/Lower Cretaceous age. The age of group A1 is less precise than group A2, given the lack of a precise definition of post-Permian APW paths, but the group A1 pole (Table 2) compares well with Late Jurassic/Early cretaceous paleomagnetic data from Spitsbergen (Fig. 12a) which have been obtained from well-dated, 150 Ma dolerites (Halvorsen 1989).

The various stages of fault reactivation along the Dalsfjord Fault are related to extensional top down to the west movements along a northwesterly displacement direction, hence nearly transposing the older Devonian and westerly directed stretching lineations in the foot-wall (Figs 4a, b and 6). This is inferred by the network nature of the fault breccias, magnetic lineations and the shear sense deduced from shear bands cutting the mylonite fabrics of foot-wall lithologies of the Askvoll Group.

Further evidence for regional scale Late Palaeozoic/Mesozoic normal faulting is found in the Solund area (Figs 1a and 11; Torsvik *et al.*, in preparation). Here, the Solund Fault intersects Lower Palaeozoic ophiolitic rocks overlain by Devonian sediments and finally truncates the Devonian rocks in Eastern Solund. Sheared Devonian conglomerates and basement rocks of the hanging-wall display gently dipping foliation planes with southeast plunging lineations (Fig. 11). Conversely, foot-wall mylonites, which are variably overprinted by later brecciation, show northwest plunging lineations. The change in foliation dips of the hanging-wall toward the contact (e.g. site 9) coincident with a change from southeast to northwest plunging lineations may be interpreted as resulting from a *normal* drag flexure. A primary unconformity has been identified at the base of the Devonian (Fig. 11), along part of the southern margin of the Solund massif (UTM 23 789), by two of the authors (THT and BAS). The presence of this unconformity places restraints on the magnitude of displacements of the Solund Fault and shows that the fault is unlikely to be a major detachment as claimed by Norton (1986) and Seguret *et al.* (1989). Indeed, it is likely that none of the low-angle faults at or near the base of the Devonian sediments in southwest Norway was the major

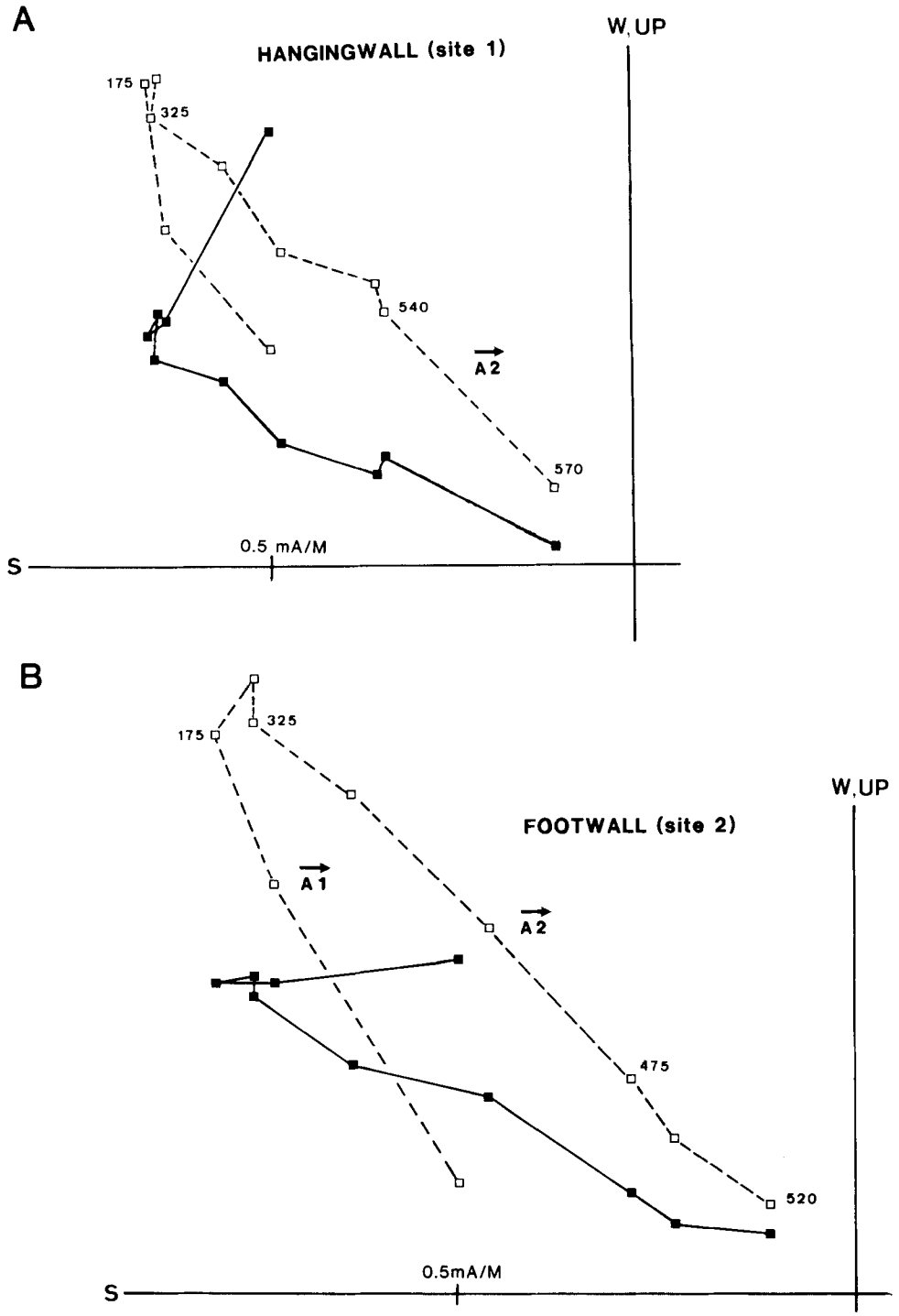

Figure 7. Typical examples of thermal demagnetization behaviour for (a) a hanging-wall mangerite breccia sample and (b) a foot-wall greenstone breccia sample. In orthogonal vector plots, closed (open) symbols represent points in the horizontal (vertical) plane.

detachment, and that the main detachment structure is probably lower in the metamorphic pile (Dewey *et al.* 1992). The unconformity close to the Solund Fault locally shows evidence for tectonic reactivation or shearing (Fig. 11, site 21b). The palaeomagnetic data from Solund are complex (Torsvik *et al.*, in preparation), but the dominating remanence component conforms to group A2 identified along the Dalsfjord Fault.

CONCLUSION AND DISCUSSION

Fault rocks in the Dalsfjord area provide clear evidence for a transition from ductile to brittle deformation, previously interpreted as representing retrograde Devonian extensional deformation. We have demonstrated, however, that at least some brittle deformation or reactivation of the upper crust occurred much later than this.

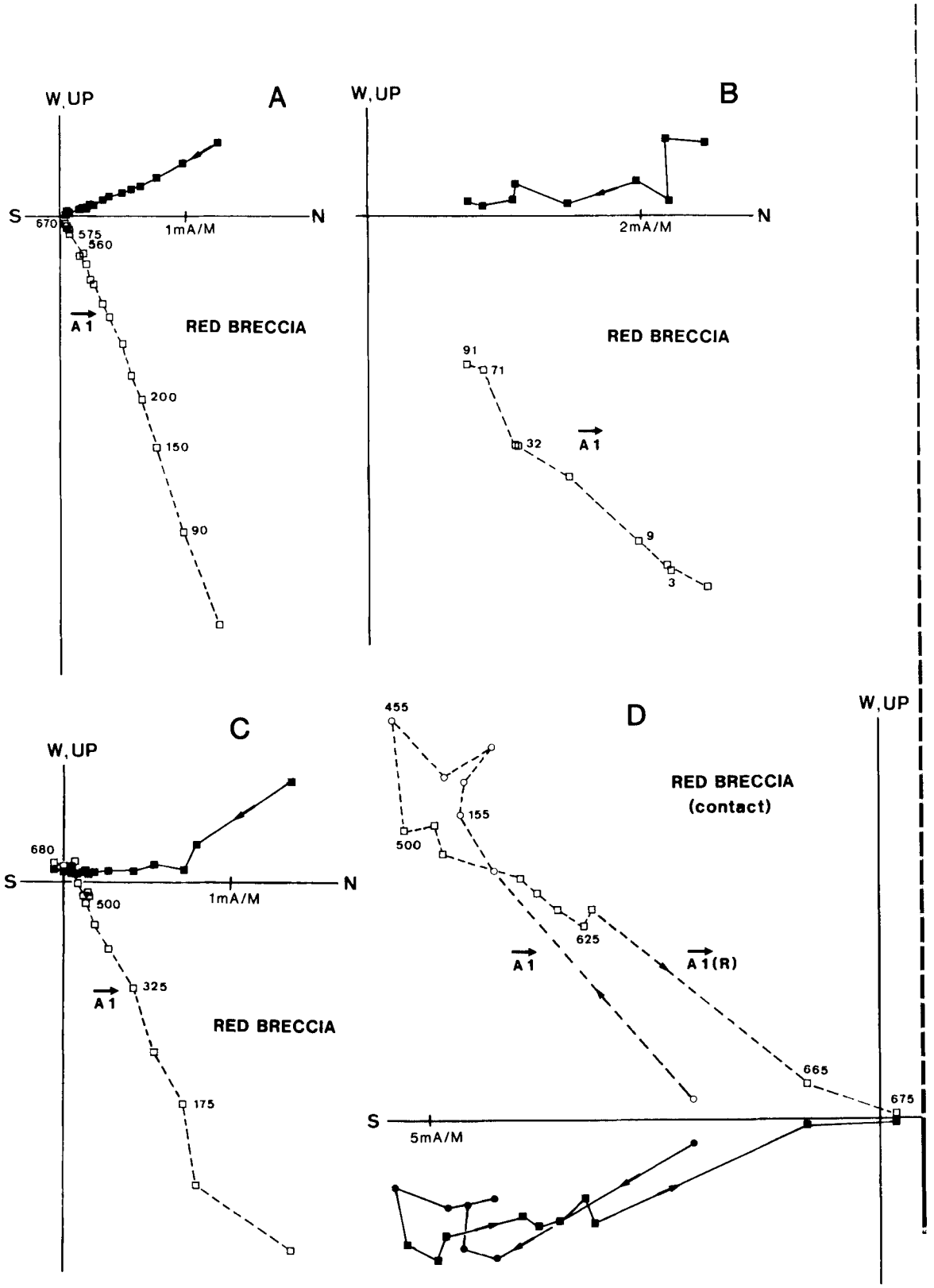

Figure 8. Examples of (a, c and d) thermal and (b) AF demagnetization behaviour for red breccia samples.

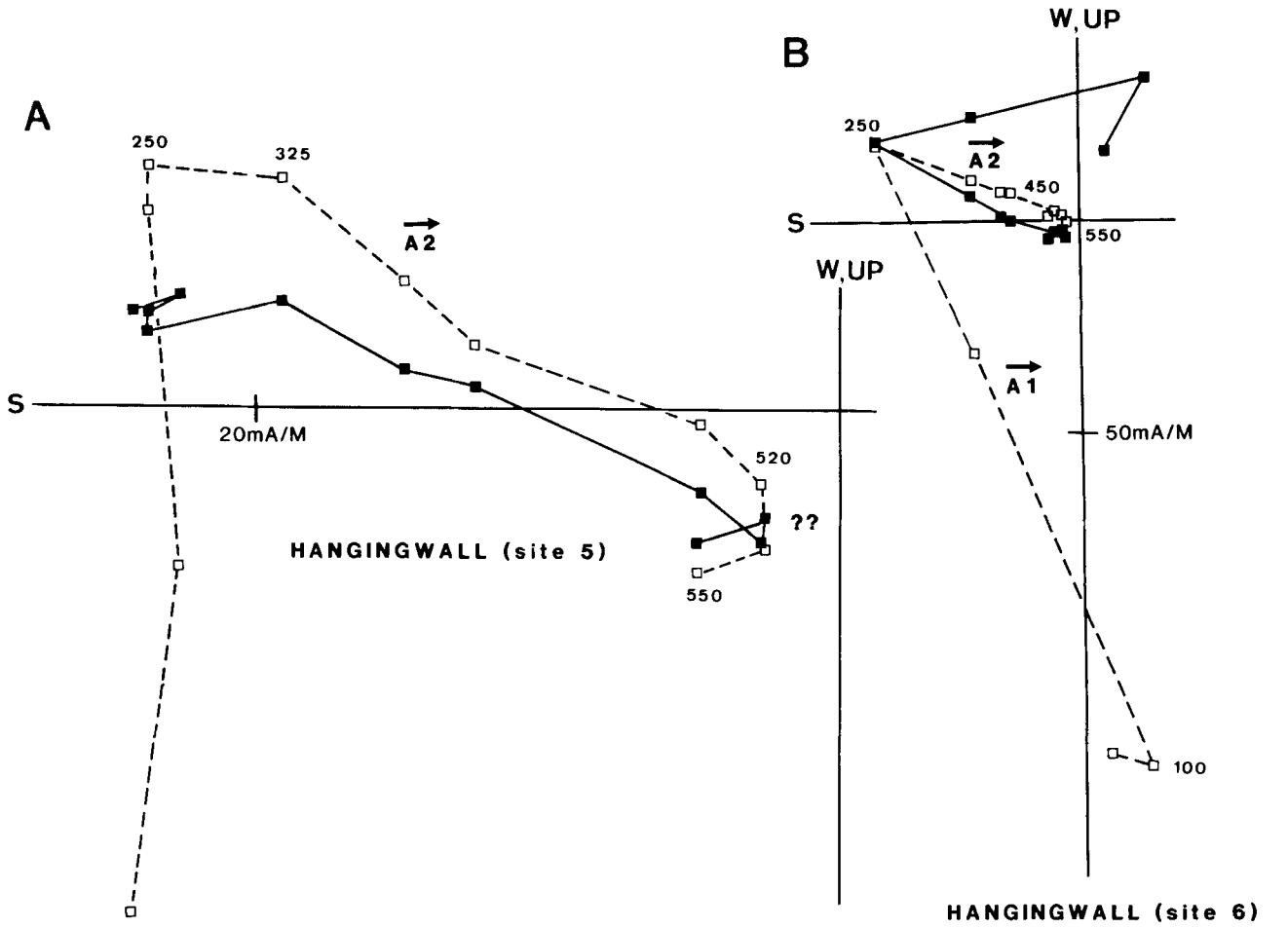

Figure 9. Examples of thermal demagnetization behaviour for hanging-wall samples from (a) site 5 and (b) site 6.

On Atløy, the Dalsfjord Fault with its conspicuous red breccia represents a low-angle Upper Jurassic/Lower Cretaceous brittle normal fault that cuts an older Permian network breccia, and also clearly truncates steeply dipping and folded Devonian extensional fabrics. The group A2 magnetizations (*c.* 250–260 Ma) are related to brecciation and metasomatism, and the Permian age suggests that this stage of reactivation of the Dalsfjord and Solund Faults coincided with regional extension during the initiation of the Viking Graben System (Ziegler 1982; Coward 1986; Brekke & Riis 1987; Beach, Bird & Gibbs 1987). K/Ar (whole rock) dating of an ultrapotassic syenite dyke within the Dalsfjord Nappe gave ages between 256 ± 6 and 261 ± 6, probably related to early magmatic activity associated with rifting in the North Sea (Furnes *et al.* 1982).

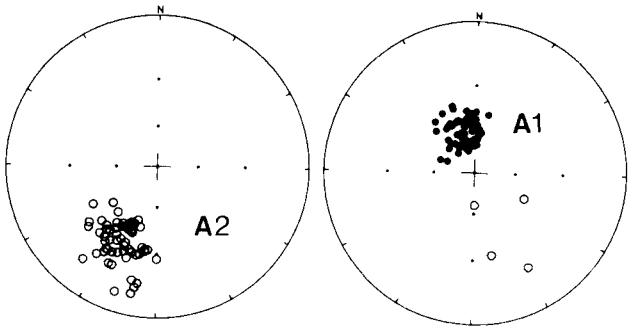

Figure 10. Distribution of characteristic remanence components derived from the Atløy and Askvoll area (equal-angle stereoplot). Group A1 is the high unblocking component in the late red breccia or the low unblocking component observed in the older fault rocks. A2 is only observed in the older breccias.

In the later red breccia on Atløy, the suggested Late Jurassic/Early cretaceous Group A1 magnetization (*c.* 150 Ma) probably was the result of low-temperature chemical changes producing a thermochemical (TCRM) magnetization in the fault zone, provided by fluids expelled into the hanging-wall breccias and partly causing magnetic resetting. Non-overlapping blocking spectra (see, e.g., Fig. 9b) may suggest local partial thermoremanent magnetic overprinting with fluid temperatures of approximately 200 °C. The timing of this brittle faulting coincides with a major stage of rifting in the Møre-Trøndelag Platform (Brekke & Riis 1987) and the Central North Sea (Hellinger, Sclater & Giltnert 1989).

An outstanding problem of extensional tectonics is that many normal faults, both planar and listric with large displacements and associated shear strains, dip at angles much less than 45° over large areas. Such extensional

Table 2. Palaeomagnetic results from sites which delineated characteristic remanence components (see text).

Site	US	maxT	Dec	Inc	N	a95	k	ReGr
Site 1								
Network Breccia (Hangingwall)	LB	208°C	323	+64	6	17.1	32	**A1**
	HB	560°C	208	-34	21	5.0	42	**A2**
Upper Contact Red Breccia	HB	670°C	151	-44	4	32.5	9	**A1**
	HB*	680°C	348	+58	38	3.4	48	**A2**
Network Breccia (Footwall)	HB	565°C	214	-36	9	5.1	86	**A2**
Site 2								
Footwall	LB	200°C	015	+63	11	4.4	107	**A1**
	HB	540°C	203	-44	11	1.3	1204	**A2**
Site 5								
Hangingwall	LB		not defined					??
	IB	499°C	196	-29	9	7.9	44	**A2**
	HB	570°C	not defined					??
Site 6								
Hangingwall	LB	240°C	337	+61	12	5.1	74	**A1**
	IB	491°C	198	-16	8	9.7	33	**A2**
	HB		not defined					??
Site 7								
Footwall	LB		not defined					??
	HB	575°C	210	-33	5	12.4	39	**A2**

Final statistics:

GROUP A1	342	+58	61	3.2	33.6		
pole:N64.8, E219.5 & dp/dm=3/5							
GROUP A2	205	-33	63	3.2	32.5		
pole:N43.2, E151.5 & dp/dm=2/4							

US=Unblocking spectra; maxT=maximum unblocking temperature;
Dec=Mean Declination; Inc=Mean Inclination; N=Number of samples;
a95=95 percent confidence circle; k=precision parameter (Fisher 1953);
ReGr=Remanence group classification.
dp/dm=semi-axis of the oval of the 95% confidence about the mean pole.

detachments are well studied in the Basin and Range tectonic province in western North America (Davis, Lister & Reynolds 1986; Gans *et al.* 1985; Holm & Wernicke 1989; Miller, Gans & Garing 1983; Miller & John 1988; Stewart 1983). This appears to defy Anderson's Law (Anderson 1942), which predicts that active normal faults should dip at more than 45°, yet seismicity and earthquake nodal plane solutions show that active normal faults in the brittle seismogenic upper crust, where Byerlee's law (Byerlee 1978; Meissner & Strehlau 1982) dominates, typically dip at more than 50° (Jackson 1987) and satisfy the predicted Mohr–Navier–Coulomb relationship.

Many low-angle normal faults clearly nucleated on older gently dipping listric thrusts (Allmendinger *et al.* 1983, 1987; Anovits & Chase 1990; Blundell, Reston & Stein 1989; Brooks, Trayner & Trimble 1988; Dalziel & Brown 1989; Jolivet *et al.* 1990; McClelland & Isachsen 1986; Pluijm & Carlson 1989; Root 1990; Wernicke 1981) showing that the coefficient of sliding friction on surfaces as much as 50° from the theoretical surfaces of maximum shearing stress modified by internal or sliding friction can be sufficiently low to allow slip (Price 1966). The low-angle extensional Kvamshesten Detachment probably nucleated in early Devonian times on an earlier gently dipping Scandian (Silurian) thrust and was reactivated as a brittle low-angle fault. Similarly, the gently dipping western bounding normal fault of the Newark Graben, in eastern Pennsylvania, reactivated, during Triassic times in the brittle regime, a late Palaeozoic thrust mylonite zone (Ratcliffe *et al.* 1986).

The planar rotational and listric explanations of low-angle normal faults do not, however, explain the virtual absence of seismic evidence of extensional slip on low-angle surfaces excepting the example documented by Eyidogan & Jackson (1985). Active extension today is not a widespread tectonic style [e.g. Basin and Range, Aegean, Tibet, and East Africa, where seismicity is on faults dipping at greater than about 50° to depths of about 15 km (Parry & Bruhn 1986, 1987; Smith & Sbar 1974; Stein & Barrientos 1985)], unlike, for example, the early Mesozoic when continental extension was globally pervasive.

A solution to this difficulty was outlined by Buck (1988) from numerical modelling and by Hamilton (1988) from geological mapping of the Panamint Detachment in the southern Basin and Range. The model involves an antilistric genetic sequential relationship between a planar irrotational steeply dipping active normal fault and a flat-lying 'dead' detachment with an intervening rollover through which the foot-wall is progressively drawn, uplifted and rotated, at once reconciling in one model the two apparently disparate elements of extension, seismic steeply dipping normal faults

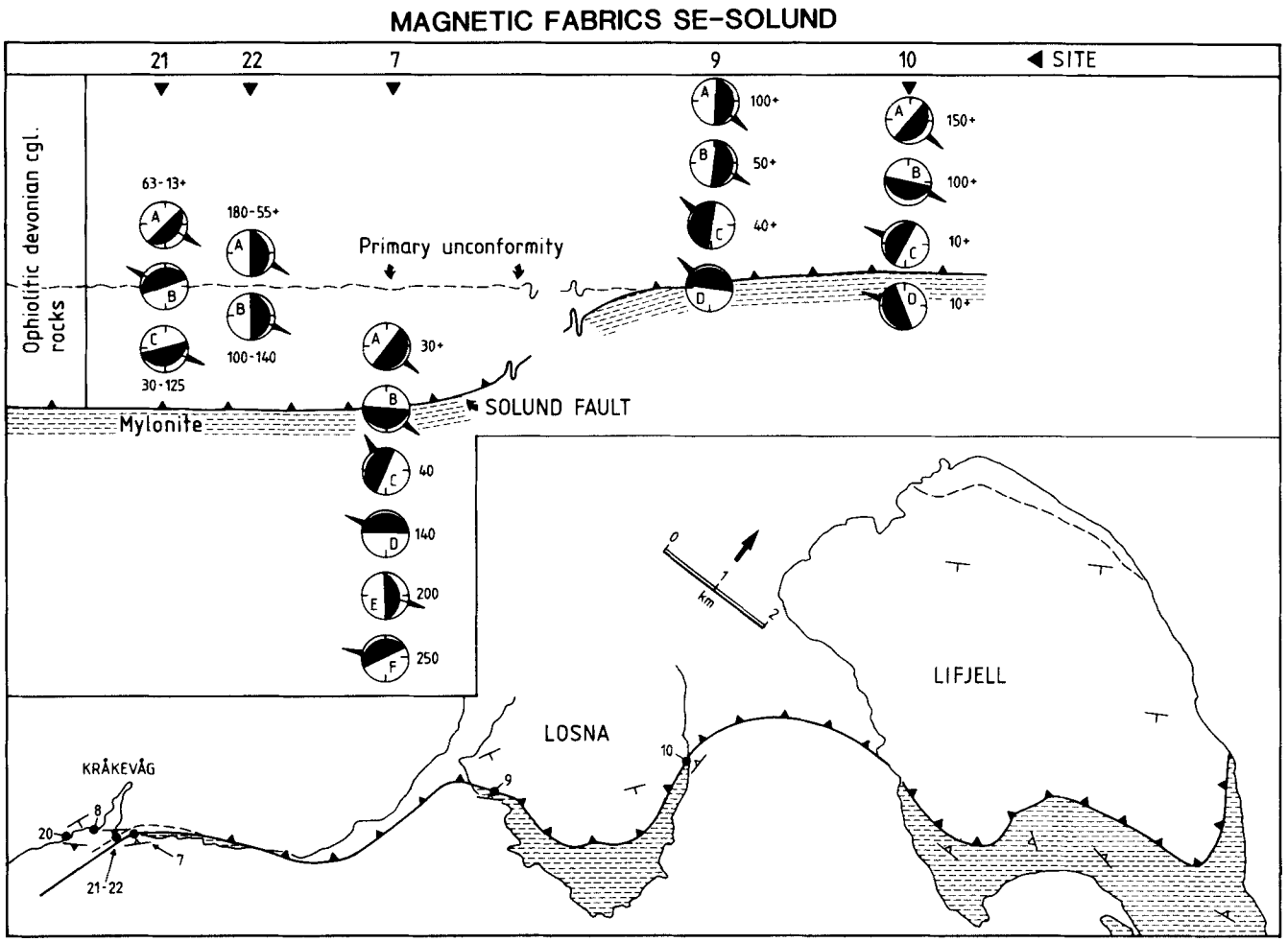

Figure 11. Geological sketch-map of the southern margin of the Solund Fault (see Fig. 1; Torsvik *et al.*, in preparation). Downward dipping magnetic foliation planes along with magnetic lineations (arrows) are shown. Numbers adjacent to stereoplot refer to distance above/below the primary unconformity (sites 21–22) or above/below the Solund Fault (sites 7, 9–10).

and aseismic gently dipping normal faults. Flat detachments of up to 80 km are believed to have been withdrawn as foot-walls to the steeply dipping seismic segment (Hamilton 1988; Dewey *et al.* 1992).

There appear to be three independent styles of low-angle normal faulting each of which penetrates the seismogenic layer in tectonic regions of high heat flow such as orogenic extensional collapse zones. Type 1 comprises rotational planar arrays (shelf of book systems) where fault spacing is about the thickness of the seismogenic layer (*c.* 10–15 km) and blocks behave as almost rigid prisms as in large areas of the modern Basin and Range (Smith & Sbar 1974) and in the Aegean region (Jackson 1987). Type 2 comprises detachments nucleated on earlier listric thrusts or other gently inclined zones of crustal weakness in the basement such as the Dalsfjord (Dalsfjord Fault is the top surface of the Kvamshesten Detachment zone) and Hornelen Detachments (Andersen & Jamtveit 1990) and the Sevier Detachment (Allmendinger *et al.* 1983). Type 3 is foot-wall rollup detachments of 80 km or more between individual faults where upper crustal blocks between faults are able to distort flexurally.

The Dalsfjord Fault clearly evolved as a Type 2 structure, from its inception as a gently dipping Scandian thrust, by successive extensional low-angle normal fault rejuvenations, the first as a phase of ductile early Devonian extensional detachment (Kvamshesten Detachment) and then brittle low-angle normal fault (Dalsfjord Fault) in Permian and mid-Mesozoic times. The importance of the Permian and Mesozoic phases of reactivation is that they demonstrate that not all active normal faults in the brittle upper crustal regime dip at an angle greater than 45°; the Dalsfjord Fault dips at only between 5° and 15°.

The Dalsfjord Fault breccias are related entirely to low-angle normal faulting and represent 'network' breccias, within which hydrothermal solutions could move freely through the system. The present exposed fault levels were probably developed under several kilometres of Palaeozoic and/or Mesozoic overburden, accounting for the lithification of the breccias. The magnetization age of the various breccias, effectively, although approximately, dates the stages of major normal fault movements. A similar bipolarity of magnetizations against faults has been observed in the Trondheimsfjord region (Grønlie & Torsvik 1989; Torsvik *et al.* 1989) and in other parts of Western Norway (Torsvik *et al.* 1988). The systematic study of the

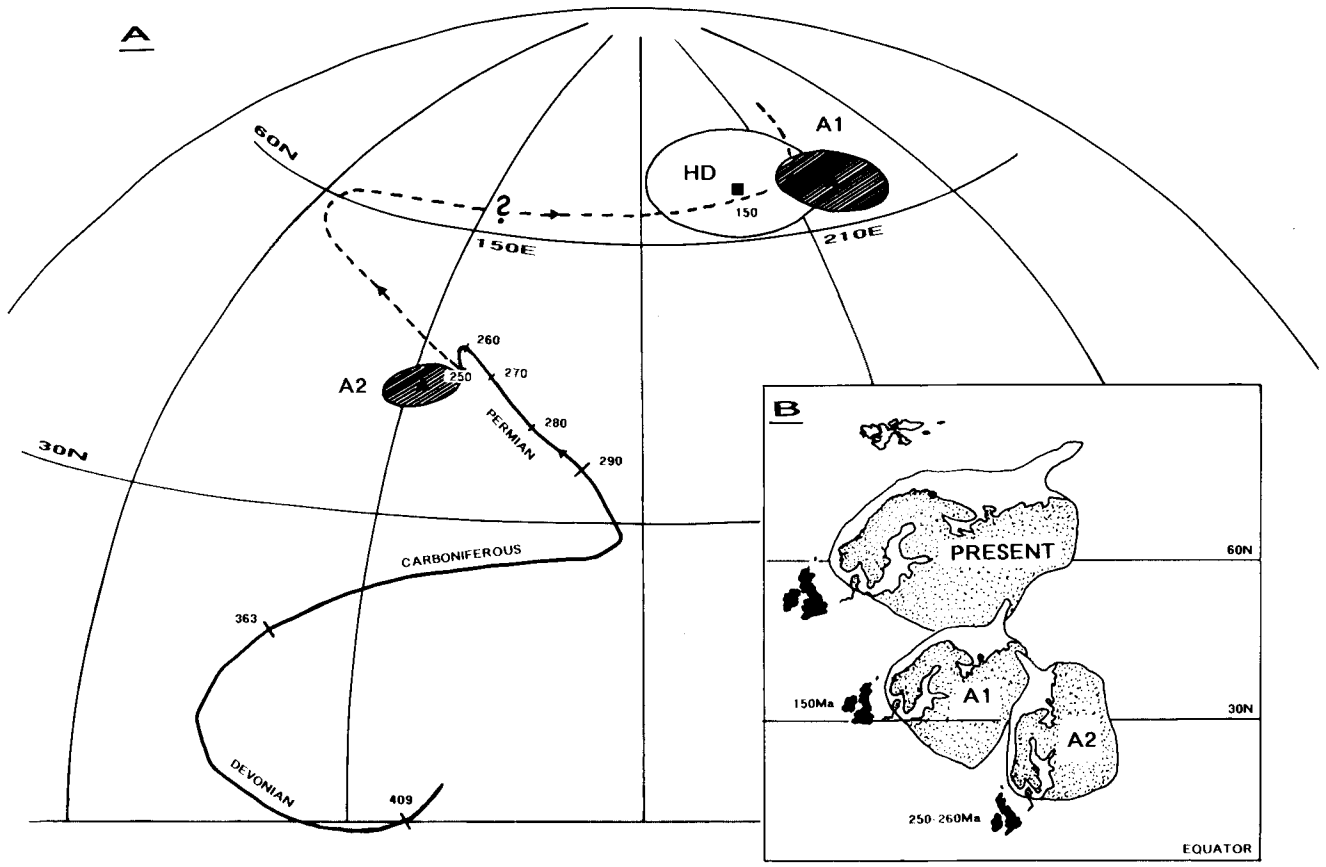

Figure 12. (a) Early Devonian to Permian (250 Ma) APW path for Baltica (Torsvik *et al.* 1992) along with the A2 and A1 poles (with *dp*/*dm* semi-axes) obtained from the breccias from Atløy. We have also included a pole from the Hinlopen dolerites (150 Ma; denoted HD in diagram), Spitsbergen (Halvorsen 1989). The post-Permian APW path is somewhat uncertain, but a suggested continuation of the path of Torsvik *et al.* (1992) is indicated (see also Torsvik *et al.* 1989). Note that A2 conform to the Permian section of the APW path (250–250 Ma), whereas the A2 pole statistically overlaps with the Hinlopen dolerite pole, suggesting an approximate age of 150 Ma. Numbers along the APW path in million years. Equal-area projection. (b) Palaeodrift history for Baltica (and the British Isles) using the A2 (250–260 Ma) and A1 (*c.* 150 Ma) poles. We have also included the present geographic position of Baltica, British Isles and Spitsbergen in the diagram. Optional longitude. Galls projection.

magnetization of relatively 'isotropic' fault rocks therefore provides important data for the dating of faults and the timing of fault reactivation.

ACKNOWLEDGMENTS

The Norwegian Research Council for the Humanities and Sciences (NAVF), Elf Aquitaine Norway and the Geological Survey of Norway (NGU) are thanked for financial support. Norwegian ILP contribution 135.

REFERENCES

Allmendinger, R. W., Sharp, J. W., Von Tish, D., Serpa, L., Brown, L., Oliver, J. & Smith, R. B., 1983. Cenozoic and Mesozoic structure of the eastern Basin and Range province, Utah, from COCORP seismic data, *Geology*, **11**, 532–536.

Allmendinger, R. W., Hauge, T. A., Hauser, E. C., Potter, C. J., Klemperer, S. L., Nelson, K. D., Kneupper, P. & Oliver, J., 1987. Overview of the COCORP 40°N Transect, western United States: the fabric of an orogenic extensional belt, *Geol. Soc. Am. Bull.* **98**, 308–319.

Andersen, T. B. & Jamtveit, B. 1990. Uplift of deep crust during orogenic extensional collapse: A model based on field studies in the Sogn–Sunnfjord region of Western Norway, *Tectonics*, **9**, 1097–1111.

Andersen, T. B., Jamtveit, B., Austrheim, H. & Dewey, J. F., 1991. Subduction and education of continental crust; major mechanisms during continental collision and orogenic extentional collapse, *Terra Nova*, **3**, 303–310.

Anderson, E. M., 1942. *The Dynamics of Faulting and Dyke Formation with Application to Britain*, Oliver & Boyd, Edinburgh.

Anovitz, L. M. & Chase, C. G., 1990. Implications of post-thrusting extension and underplating for P–T–t paths in granulite terranes: a Grenville example, *Geology*, **18**, 466–469.

Beach, A., Bird, T. & Gibbs, A., 1987. Extensional tectonics and crustal structure: deep seismic reflection data from the northern North Sea Viking graben, in *Continental Extentional Tectonics*, Geological Society of London Special Publication, vol. 28, pp. 467–476, eds Coward, M. P., Dewey, J. F. & Hancock, P. L.

Blundell, D. J., Reston, T. J. & Stein, A. M., 1989. Deep crustal structural controls on sedimentary basin geometry, *Am. geophys. Un. geophys. Mono.*, **48**, 57–64.

Brekke, H. & Riis, F., 1987. Tectonics and basin evolution of the

Norwegian shelf between 62°N and 72°N, *Norwegian Petrol. Directorate Contrib.*, **25,** 1–17.

Brekke, H. & Solberg, P., 1987. The geology of Atløy, Sunnfjord, western Norway, *Norsk Geologiske Undersøkelse,* **410,** 73–94.

Brooks, M., Trayner, P. M. & Trimble, T. J., 1988. Mesozoic reactivation of Variscan thrusting in the British Channel area, UK, *J. geol. Soc. Lond.*, **145,** 439–444.

Buck, W. R., 1988. Flextural rotation of normal faults, *Tectonics,* **7,** 959–973.

Byerlee, J. D., 1978. Friction of rocks, *Pure appl. Geophys.*, **116,** 615–626.

Coward, M., 1986. Homogeneous stretching, simple shear and basin development, *Earth planet. Sci. Lett.*, **80,** 325–336.

Dalziel, I. W. D. & Brown, R. L., 1989. Tectonic denudation of the Darwin metamorphic core complex in the Andes of Tierra del Fuego, southernmost Chile: implications for Cordilleran orogenesis, *Geology,* **17,** 699–703.

Davis, G. A., Lister, G. S. & Reynolds, S. J., 1986. Structural evolution of the Whipple and South mountains shear zones, southwestern United States, *Geology,* **14,** 7–10.

Dewey, J. F., Andersen, T. B. & Hamilton, W. B., 1992. Extensional detachments: their origin, characteristics and distribution, *Basin Res.*, in press.

Eyidogan, H. & Jackson, J. A., 1985. A seismological study of normal faulting in the Demirci, Alasehir and Gediz earthquakes of 1969–70 in western Turkey: implications for the nature and geometry of deformation in the continental crust, *Geophys. J. R. astr. Soc.*, **81,** 569–608.

Fisher, R. A., 1953. Dispersion on a sphere, *Proc. R. Soc. Lond.*, A, **217,** 295–305.

Furnes, H., Mitchell, J. G., Robins, B., Ryan, P. D. & Skjerlie, F. J., 1982. Petrography and geochemistry of peralkine, ultrapotassic syenite dykes of Middle Permian age, Sunnfjord, West Norway, *Norsk Geologisk Tidsskrift,* **62,** 147–159.

Gans, P. B., Miller, E. L., McCarthy, J. & Ouldcott, M. L., 1985. Tertiary extensional faulting and evolving ductile–brittle transition zones in the northern Snake Range and vicinity: new insights from seismic data, *Geology,* **13,** 189–193.

Grønlie, A. & Torsvik, T. H., 1989. On the origin and age of hydrothermal thorium-enriched carbonate veins and breccias in the Møre–Trøndelag Fault Zone, central Norway, *Norsk Geologisk Tidsskrift,* **69,** 1–19.

Halvorsen, E., 1989. A palaeomagnetic pole position of Late Jurassic/Early Cretaceous dolerites from Hinlopenstretet, and its tectonic implications, *Earth planet. Sci. Lett.*, **94,** 398–408.

Hamilton, W. B., 1988. Detachment faulting in the Death Valley Region, California and Nevada, *US geol. Surv. Bull.*, **1790,** 51–85.

Hellinger, S. J., Sclater, J. G. & Giltnert, J., 1989. Mid-Jurassic through mid-Cretaceous extension in the central Graben of the North Sea—part 1: estimates from subsidence, *Basin Res.*, **1,** 191–200.

Holm, D. K. & Wernicke, B. P., 1989. Are the Black Mountains, Death Valley, CA, a 15–30 km crustal section? *Geol. Soc. Am. Abstr.*, **21,** 353.

Hossack, J. R., 1984. The geometry of listric growth faults in the Devonian Basins of Sunnfjord, West Norway, *J. geol. Soc. Lond.*, **141,** 629–638.

Høysæter, T., 1971. Thrust Devonian sediments in the Kvamshesten area, Western Norway, *Geol. Mag.*, **108,** 287–292.

Jackson, J. A., 1987. Active normal faulting and crustal extension, *Geol. Soc. Lond. Spec. Publ.*, **28,** 3–17.

Jolivet, L., Dubois, R., Fournier, M., Goffe, B., Michard, A. & Jourdan, C., 1990. Ductile extension in Alpine Corsica, *Geology,* **18,** 1007–1010.

McClelland, J. M. & Isachsen, Y. W., 1986. Synthesis of geology of the Adirondack Mountains, New York, and their tectonic setting with the southwestern Grenville Province, *Geol. Assoc. Can. Spec. Paper,* **31,** 75–94.

Meissner, R. & Strehlau, J., 1982. Limits of stresses in continental crust and their relationship to depth of shallow earthquakes, *Tectonics,* **1,** 73–79.

Miller, J. M. G. & John, B. E., 1988. Detached strata in a Tertiary low-angle normal fault terrane, southeastern California: a sedimentary record of unrofing, breaching and continental slip, *Geology,* **16,** 656–648.

Miller, E. L., Gans, P. B. & Garing, J., 1983. The Snake Range decollement: an exhumed mid-Tertiary brittle–ductile transition, *Tectonics,* **2,** 239–263.

Nilsen, T. H., 1968. The relationship of sedimentation to tectonics in the Solund Devonian district of southwestern Norway, *Norges Geologiske Undersøkelse,* **259,** 1–108.

Norton, M., 1986. Late Caledonide extension in western Norway: a response to extreme crustal thickening, *Tectonics,* **5,** 195–204.

Parry, W. T. & Bruhn, R. L., 1987. Fluid inclusion evidence for minimum 11 km offset on the Wasatch Fault, Utah, *Geology,* **15,** 67–70.

Pluijm, B. A. van der & Carson, K. A., 1989. Extension in the central metasedimentary belt of the Ontario Grenville: timing and tectonic significance, *Geology,* **17,** 164.

Price, N. J., 1966. *Fault and Joint Development in Brittle and Semi-Brittle Rocks,* Pergamon Press, Oxford.

Ratcliffe, N. M., Burton, W. C., D'Angelo, R. M. & Costain, J. K., 1986. Low-angle extensional faulting, reactivated mylonites, and seismic reflection geometry of the Newark basin margin in eastern Pennyslvania, *Geology,* **14,** 766–770.

Roberts, D., 1983. Devonian tectonic deformation in the Norwegian Caledonides and its regional perspective, *Norges Geologiske Undersøkelse,* **359,** 43–60.

Roddom, D. S., Miller, J. A. & Flinn, D., 1989. Permo-Carboniferous mylonite formation in the Walls Boundary Fault system, Shetland, *Proc. Yorkshire geol. Soc.*, **47,** 339–343.

Root, K. G., 1990. Extensional duplex in the Purcell Mountains of southeastern British Columbia, *Geology,* **18,** 419–421.

Seguret, M., Seranne, M., Chauvet, A. & Brunel, M., 1989. A new type of extensional sedimenatry basin from the Devonian of Norway, *Geology,* **17,** 127–130.

Seranne, M. & Seguret, M., 1987. The Devonian Basins of western Norway: Tectonics and kinematics of an extended crust, in *Continental Extensional Tectonics,* Geological Society of London Special publication, vol. 28, pp. 537–548, eds Coward, M. P., Dewey, J. F. & Hancock, P. L.

Skjerlie, F. J., 1969. The pre-Devonian rocks in the Askvoll–Gaular area and adjacent districts, Western Norway, *Norges Geologiske Undersøkelse,* **258,** 325–359.

Skjerlie, F. J., 1971. Sedimentasjon og tektonisk utvikling i Kvamshesten Devonfelt, Vest Norge, *Norges Geologiske Undersøkelse,* **302,** 77–108.

Skjerlie, F. J., 1974. The Lower Palaeozoic sequence of the Stavfjord district, Sunnfjord, *Norges Geologiske Undersøkelse,* **302,** 1–32.

Smith, R. B. & Sbar, M. L., 1974. Contemporary tectonics and seismicity of the Western United States with emphasis on the Intermountain Seismic Belt, *Geol. Soc. Am. Bull.*, **85,** 1205–1218.

Stein, R. S. & Barrientos, S. E., 1985. Planar high-angle faulting in the Basin and Range. Geodetic analysis of the 1983 Borah Peak, Idaho, Earthquake, *J. geophys. Res.*, **90,** 11 355–11 366.

Stewart, J. H., 1983. Extensional tectonics in the Death Valley area, California: transport of the Panamint Range structural block 80 km northwestward, *Geology,* **11,** 153–157.

Sturt, B. A., 1983. Late Caledonian and possible Variscan stages in the Orogenic evolution of the Scandinavian Caledonides, *The Caledonide Orogen—IGCP Project 27,* Symposium de Rabat, Morocco (abstract).

Swensson, E. & Andersen, T. B., 1991. Petrography and

basement-cover relationships between the Askvoll Group and the Western Gneiss Region (WGR), Sunnfjord, W. Norway, *Norsk Geologisk Tidsskrift*, **71**, 15–27.

Torsvik, T. H., Sturt, B. A., Ramsay, D. M. & Vetti, V., 1987. The tectonomagnetic signature of the Old Red Sandstone and pre-Devonian strata in the Håsteinen area, Western Norway, and implications for the later stages of the Caledonian Orogeny, *Tectonics*, **6**, 305–322.

Torsvik, T. H., Smethurst, M., Briden, J. C. & Sturt, B. A., 1990. A review of Palaeozoic palaeomagnetic data from Europe and their palaeogeographical implications, in *Palaeozoic Palaeogeography and Biogeography*, Geological Society of London Memoir, vol. 12, pp. 25–41, eds McKerrow, W. S. & Scotese, C. R.

Torsvik, T. H., Sturt, B. A., Ramsay, D. M., Kisch, H. J. & Bering, D., 1986. The tectonic implications of Solundian (Upper Devonian) magnetization of the Devonian rocks of Kvamshesten, Western Norway, *Earth planet. Sci. Lett.*, **80**, 337–347.

Torsvik, T. H., Sturt, B. A., Ramsay, D. M., Bering, D. & Fluge, P., 1988. Palaeomagnetism, the Magnetic Fabrics and the structural style of the Hornelen Old Red Sandstone, Western Norway, *J. geol. Soc. Lon.*, **145**, 413–430.

Torsvik, T. H., Smethurst, M. A., Van der Voo, R., Trench, A., Abrahams, N. & Halvorsen, E., 1992. BALTICA—A synopsis of Vendian–Permian palaeomagnetic data and their palaeotectonic implications, Earth Science Reviews, submitted.

Torsvik, T. H., Sturt, B. A., Ramsay, D. M., Grønlie, A., Roberts, D., Smethurst, M., Atakan, K., Bøe, R. & Walderhaug, H. J., 1989. Palaeomagnetic constraints on the early history of the Møre–Trøndelag Fault Zone, Central Norway, in *Palaeomagnetic Rotations and Continental Deformation*, Nato ASI series, vol. C254, 431–457, eds Kissel, C. & Laj, C., Kluwer Academic Publishers, Dordrecht.

Wernicke, B. P., 1981. Low-angle normal faults in the Basin and Range Province: nappe tectonics in an extending orogen, *Nature*, **291**, 656–648.

Ziegler, P., 1982. *Geological Atlas of Western and Central Europe*, Shell, The Hague.